

Pérez-Trujillo et al., 2017

Volume 3 Issue 2, pp. 145-164

Date of Publication: 18<sup>th</sup> September 2017

DOI-<https://dx.doi.org/10.20319/mijst.2017.32.145164>

This paper can be cited as: Pérez-Trujillo, J., Kowalski, G., & Elizalde-Blancas, F. (2017). Transient Analysis of a Compressed Air Energy Storage System. *MATTER: International Journal of Science and Technology*, 3(2), 145-164.

This work is licensed under the Creative Commons Attribution-Non Commercial 4.0 International License. To view a copy of this license, visit <http://creativecommons.org/licenses/by-nc/4.0/> or send a letter to Creative Commons, PO Box 1866, Mountain View, CA 94042, USA.

## TRANSIENT ANALYSIS OF A COMPRESSED AIR ENERGY STORAGE SYSTEM

**Juan Pedro Pérez-Trujillo**

University of Guanajuato, DICIS, Mechanical Engineering Department, Carretera Salamanca-Valle de Santiago, km. 3.5+1.8, Palo Blanco, Salamanca, Guanajuato, 36885, Mexico

[jp.pereztrujillo@hotmail.com](mailto:jp.pereztrujillo@hotmail.com)

**Gregory J. Kowalski**

Northeastern University, 360 Huntington Avenue, Boston, Massachusetts 02115, USA

[gkowal@coe.neu.edu](mailto:gkowal@coe.neu.edu)

**Francisco Elizalde-Blancas**

University of Guanajuato, DICIS, Mechanical Engineering Department, Carretera Salamanca-Valle de Santiago, km. 3.5+1.8, Palo Blanco, Salamanca, Guanajuato, 36885, Mexico

[franciscoeb@ugto.mx](mailto:franciscoeb@ugto.mx)

---

### Abstract

*A transient energy analysis was performed in a Compressed Air Energy Storage (CAES) system. The aim is to perform a parametric analysis to determine the efficiency and output energy depending on some design parameters as the number of tanks connected in parallel, the insulation thickness, the storage time and the outflow. Mass and energy balances were carried out on every component of the system, the resulting equations from the analysis were solved numerically using the explicit Euler's method. The system operating for a short storage time presents a higher efficiency (about 42.38%) with insulated tanks, however it is lower (about 23.54%) for long storage time and non-insulated tanks. Nevertheless, when the system with*

*insulated tanks reaches the steady state, i.e., for long storage time, its efficiency is almost half that one with tanks without insulation, 11.5% and 23.54%, respectively. These results indicate that for short storage times is better to insulate the tanks and for longer storage times is more convenient no insulation.*

### **Keywords**

Transient Analysis, CAES, Energy Storage, Numerical Solution, Compressor, Turbine

---

## **1. Introduction**

The network power reliability is facing a great challenge with the rapid increase of intermittent renewable energy integration, the biggest challenge is filling the gap between production, storage and availability for the end user (Zhao, Wu, Hu, Xu, & Rasmussen, 2015), (Akinyele & Rayudu, 2014), (Beaudin, Zareipour, Schellenberglobe, & Rosehart, 2010), (Budt, Wolf, Span, & Yan, 2016), (Charan, Laxmi, & Sangeetha, 2017), (Soltan & Thorman, 2017). Various Electrical Energy Storage (EES) technologies offer technical and economic benefits from generation, transmission and distribution to demand side management. Several options for converting electricity to stored energy have been demonstrated, these include batteries, pumped hydroelectric storage (PHES) and compressed air energy storage (CAES) in caverns or other reservoirs. CAES systems are distinguished as large-scale, low cost, long lifetime and good established operation experience compared with other energy storage methods. CAES is considered as one of the cheapest EES technologies in terms of capital cost (\$/kWh) and maintenance cost (\$/kW-year) (Akinyele & Rayudu, 2014), (Luo, et al., 2016), (Shakeri, Soltanzadeh, Berson, & Sharp, 2014). CAES systems work during the periods of low power demand, the surplus electricity drives a motor/generator unit in turn to run a compressor in order to inject air into a storage vessel, which can be an underground cavern or above ground tank. In this way the energy is stored as high pressure air. When the power generation cannot meet the load demand, the stored compressed air is released through a turbine-generator system arrangement to provide the necessary electricity. The most of the energy losses in CAES systems occur during the compression and storage air processes, so reducing significantly the turbine efficiency. To improve the efficiency during the expansion process, the compressed air can be heated using the combustion of fossil fuels or heat recovery from the compressor process, then the compressed heated air is fed to turbines which deliver mechanical power, which is finally converted again in electricity using an electric generator. To increase the efficiency of CAES

systems, the waste heat from the turbine exhaust can be recycled by a recuperation unit (Luo, et al., 2016), (Shakeri, Soltanzadeh, Berson, & Sharp, 2014), (Luo, Wang, Dooner, & Clarke, 2015), (Zhao, Wu, Hu, Xu, & Rasmussen, 2015), (Beaudin, Zareipour, Schellenberglabe, & Rosehart, 2010). The major concern in deployment of CAES systems is its relatively low cycle efficiency compared with other EES technologies. With the goal of improving CAES efficiency and avoiding the use of fossil fuels, the Adiabatic CAES (A-CAES) system concept was proposed. A-CAES combined with Thermal Energy Storage (TES) is designed to extract heat from the stage of air compression and store it in an adiabatic reservoir. The heat is then reused before the air expansion and electricity generation process (Luo, et al., 2016), (Shakeri, Soltanzadeh, Berson, & Sharp, 2014), (Luo, Wang, Dooner, & Clarke, 2015), (Zhao, Wu, Hu, Xu, & Rasmussen, 2015), (Beaudin, Zareipour, Schellenberglabe, & Rosehart, 2010). This work is focused in a transient energy analysis of every component to give a better understanding of the performance of a simple CAES system by the use of a numerical analysis. The system is sized to satisfy a hypothetical case of electrical demand.

## 2. Plant Configuration and Design Methodology

The CAES system, proposed in this work, is sized to satisfy the hypothetical electricity demand, which is shown in Figure 1, which is representative of a typical user consumption per day. In this case the peak load is assumed to start at 6:00 hrs and end at 19:00 hrs, while the low electrical demand period is from 19:00 hrs to 6:00 hrs. Figure 2 shows the system configuration in which the main components to be analyzed are the motor, compressor, tank or reservoir, turbine and finally the generator. The number of tanks is selected depending on the energy output and desired discharge time.

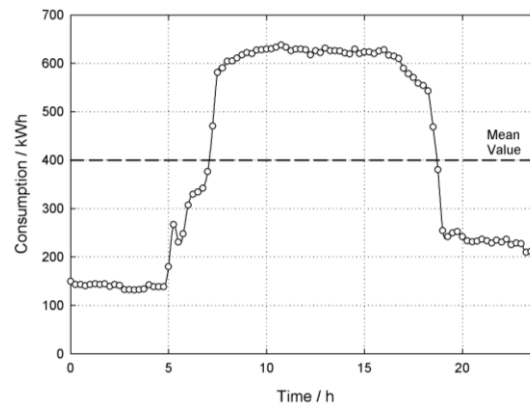
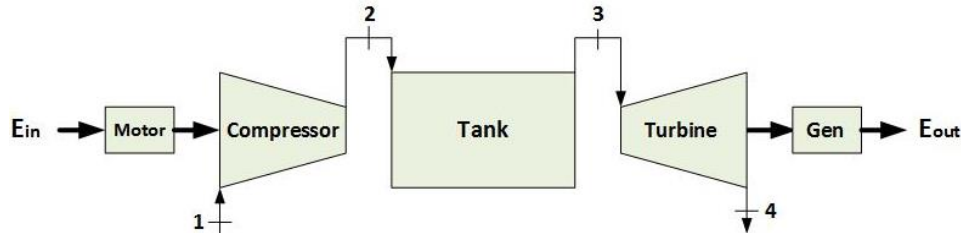


Figure 1: Example of Demand Electricity

The system is assumed to be installed over ground, without any thermal energy recovery system, also none auxiliary fuel system. The design of the system is based on an analytical procedure that has been conducted using a transient approach. The analysis includes determining the number and array of tanks, the thickness of insulation, and the outflow rate during the discharge period.



**Figure 2: CAES System Arrangement**

The main design constrains and assumptions are summarized as follows:

- The maximum and minimum pressure fo the air tank have been set.
- The maximum pressure of the tanks is limited by the selected tank design pressure.
- The minimum pressure of the tank is assumed to be  $1.25 P_{atm}$  to guarantee an outflow and in this way avoiding any damage in the turbine.
- The polytropic efficiencies of compressor, turbine, motor and electrical generator have been assigned.
- A constant value of the electrical power supplied to the system is assumed.
- Ambient conditions and inlet air have been taken at standard values.
- The gases are considered as ideal gases.

Table 1 shows the input data and constrains that were prescribed in order to size the system. The development of the mathematical model is presented in the next section. The resulting set of equations is solved using Matlab whereas the fluids properties are taken from RefPROP.

**Table 1: Operational Parameters**

Parameter	symbol	value	units
Inlet pressure, compressor	$P_1$	100	kPa
Inlet temperature, compressor	$T_1$	293	K
Outlet pressure, compressor	$P_2$	2000	kPa
Outlet pressure, turbine	$P_4$	100	kPa

Compressor isentropic efficiency	$\eta_C$	90	%
Discharge pressure	$P_D$	125	kPa
Turbine isentropic efficiency	$\eta_T$	90	%
Power supplied to motor	$E_{in}$	75	kW
Motor efficiency	$\eta_M$	95	%
Generator efficiency	$\eta_G$	90	%
Ground Temperature	$T_{GD}$	298	K
Ambient Temperature	$T_\infty$	293	K
Ambient Pressure	$P_\infty$	100	kPa

## 2.1 CAES Design Analysis

The components of the system are analyzed applying the governing equations at every thermodynamic state in order to determine the mass flow rate and the energy transfer in each process. The general equations are listed below (Moran, Shapiro, Boettner, & Bailey, 2010).

The mass balance equation:

$$\frac{dm_{cv}}{dt} = \sum \dot{m}_i - \sum \dot{m}_e \quad (1)$$

The energy balance equation:

$$\frac{dE_{cv}}{dt} = \dot{Q} - \dot{W} + \sum \dot{m}_i h_i - \sum \dot{m}_e h_e \quad (2)$$

The motor is the first component analyzed, it does not have any flow of mass but it has an input of electrical energy, energy losses by heat dissipation to the environment and transfer of energy as power out of the system.

The energy balance in the motor is stated as:

$$\dot{E}_{in} = \dot{W}_{act} + \dot{Q}_{dis} \quad (3)$$

The heat dissipated by the motor is unknown but it can be determined applying the efficiency of the motor, which is:

$$\dot{Q}_{dis} = (1 - \eta_M) \dot{E}_{in} \quad (4)$$

The electrical energy supplied to the motor is converted in mechanical energy used to move the compressor, which is considered to operate adiabatically at maximum capacity. The

inlet flow rate is considered constant, and as no other inlet is present, the outflow rate equals the inlet flow, which means that this component works in permanent state.

The power required by the compressor is stated as:

$$\dot{W}_C = \dot{m}_i (h_2 - h_1) \quad (5)$$

State 2 is defined by  $T_2$  and  $P_2$ . The temperature at state 2 depends on the isentropic efficiency of the compressor which is stated as:

$$\eta_{s,C} = \frac{T_{2s} - T_1}{T_2 - T_1} \quad (6)$$

Considering an isentropic process and an ideal gas behavior, the temperature in the compressor discharge process is stated as:

$$T_2 = \left( \frac{1}{\eta_c} \left( \left( \frac{P_2}{P_1} \right)^{\frac{k-1}{k}} - 1 \right) + 1 \right) T_1 \quad (7)$$

The tank is analyzed considering three main processes: 1) charge, storage and discharge. The charge process is characterized because the mass is being accumulated and followed by an increase of temperature and pressure. In the storage process the main characteristic is the loss of energy by heat transfer to the surroundings. Finally the discharge process occurs when the air flow is sent to the turbine decreasing the mass inside the tank followed by a reduction of pressure and temperature. In the following lines the mathematical equations that describe these phenomena are presented.

During the charge process the tank is assumed initially to be at the environmental conditions and the change of mass related to the charge time is:

$$\frac{dm_{CV}}{dt} = \dot{m}_i \quad (8)$$

The energy balance for the tank during the charge process is shown in equation (9). This equation states that the time rate change of energy inside the tank during the charge process equals the incoming energy accompanying mass flow of air minus the heat lost during the charge process.

$$\frac{dE_{CV}}{dt} = \dot{m}_i h_2 - \dot{Q} \quad (9)$$

The change of energy inside the tank depends directly on the mass of air stored and its temperature.

$$E_{CV} = m_{CV} c_v T_{\text{tank}} \quad (10)$$

In the same way, the heat lost influences strongly the temperature inside the tank. It is stated as:

$$\dot{Q} = C_{eq} (T_{\text{tank}} - T_{\infty}) \quad (11)$$

The heat losses are determined considering an effective heat transfer coefficient,  $C_{eq}$ , which is constituted by the thermal resistance by conduction through the steel and thermal insulator, and one thermal resistance to convection caused by the external convection with the environment. The effective heat transfer coefficient is calculated following the next relationship:

$$C_{eff} = \frac{A}{\frac{1}{h_i} + \frac{l_m}{k_m} + \frac{l_i}{k_i} + \frac{1}{h_o}} \quad (12)$$

In the storage process there is no mass flowing out or in the tank. There is only heat losses between the stored air and the surroundings. These energy losses are determined by the insulation quality, the environmental temperature, and the storage time. It is important to notice that if the storage time increases, the energy losses increase, so it is easier to reach thermal equilibrium between the stored air and its surroundings.

The energy balance in the tank during the storage process is stated by:

$$\frac{dE_{CV}}{dt} = -\dot{Q} = -C_{eq} (T_{\text{tank}} - T_{\infty}) \quad (13)$$

In the discharge process, for this analysis the outflow rate is considered constant during the process. In order to guarantee an airflow, the discharge will stop until the pressure in the tank reaches the value of  $1.25 P_{\text{atm}}$ . While the discharge occurs, a heat flow is transferred to the atmosphere, also a decrease in the mass, temperature and pressure inside the tank is associated.

The change in the mass can be known applying the mass balance, which is stated as:

$$\frac{dm_{CV}}{dt} = -\dot{m}_e \quad (14)$$

On the other hand, the energy balance during the discharge process is stated as:

$$\frac{dE_{CV}}{dt} = -\dot{m}_e h_e - \dot{Q} \quad (15)$$

The pressure inside the tank in every process is determined considering an ideal gas behavior knowing the temperature and the mass of air inside the tank.

$$p = \frac{m_{cv}RT}{V_T} \quad (16)$$

Following the analysis, the turbine work is assumed to be developed with constant efficiency during the power generation process. The mass flow rate through the turbine is considered constant because there is no present any loss of mass between it and its surroundings. No heat losses occur, i.e. an adiabatic process. The inlet conditions are known from the discharge process, and at the exit, the pressure is known because it is assumed that the turbine discharges to the environment, therefore, only the exit temperature is required to determine the power developed by the turbine.

After doing an energy balance in the turbine, the developed power can be determined as:

$$\dot{W}_T = \dot{m}_3 (h_3 - h_4) \quad (17)$$

The isentropic turbine efficiency is stated as:

$$\eta_{s,T} = \frac{T_3 - T_4}{T_3 - T_{4s}} \quad (18)$$

The exit temperature can be determined considering an isentropic expansion process and an ideal gas behavior. Considering the air as an ideal mixture of oxygen and nitrogen, the exit temperature can be determine as:

$$x_{O_2} s_{4,O_2}^o + x_{N_2} s_{4,N_2}^o = x_{O_2} s_{3,O_2}^o + x_{N_2} s_{3,N_2}^o + R \ln \left( \frac{P_4}{P_3} \right) \quad (19)$$

The last equipment is the electrical generator. The output electrical energy is obtained from converting the mechanical power delivered by the turbine into electrical power.

When the energy balance is performed for the generator, its power is stated as:

$$\dot{W}_{in} = \dot{E}_{out} + \dot{Q}_{dis} \quad (20)$$

When all the governing equations are set, the solution to those equations is determined by using a numerical method. The set of equations allows to calculate the rate of change of the dependent parameter, like mass and energy, to be computed as a function of the independent variable which is time. The solution to the problem is therefore a matter of integrating the governing differential equation forward in time.

The Euler's technique is used to solve the differential equations, which is an explicit numerical technique. Euler's method approximates the rate of change within the time step as being constant and equal to its value at the beginning of the time step (Klein & Nellis, 2013), (Hoffman & Frankel, 2001). Therefore, for any time step j:



$$y_{j+1} = y_j + \left. \frac{dy}{dt} \right|_{y=y_j, t=t_j} \Delta t \quad (21)$$

The value of the solution at the end of the time step ( $y_{j+1}$ ) can be calculated explicitly using information at the beginning of the time step ( $y_j$ ). The term  $dy/dt$  is computed using the governing differential equation evaluated in the previous time,  $t_j$ . The time step used in the analysis was 1 min.

### 3. Results

The parametric analysis consisted on quantifying the changes in overall system efficiency and output energy related to the number of tanks connected in parallel, the insulation thickness, the storage time and finally the outflow rate. The number of tanks were varied from one to ten in order to evaluate the parameters of interest. The tank used to size the storage system is selected from the Manchester Tank enterprise (Manchester Tank Co., 2017). The selected tank has a maximum operational pressure of 1122.4 kPa, and a capacity of 37.85 m<sup>3</sup>. The tank is made of steel and initially it does not have insulation. Firstly, the system is analyzed considering that the tanks do not have any thermal insulation, later on insulation thicknesses of 12.5 mm, 25 mm, 50 mm and 100 mm were considered. These results are presented from Figure 3 to Figure 12, for which the storage time is considered to be 30 min.

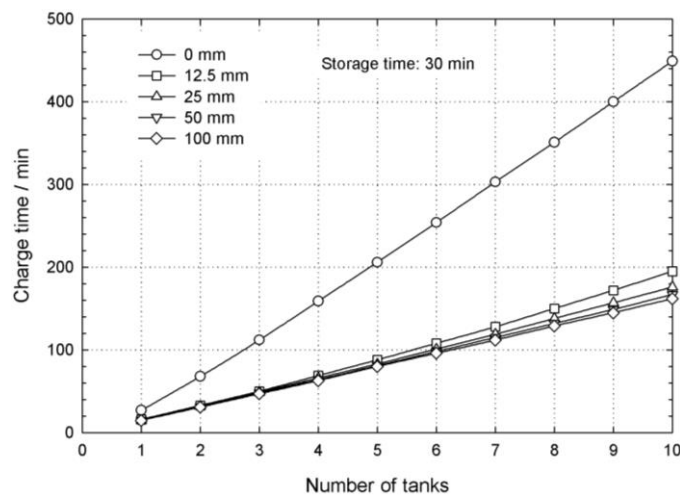


**Figure 3:** Charge time vs number of tanks for a storage time of 30 min with different insulation thickness

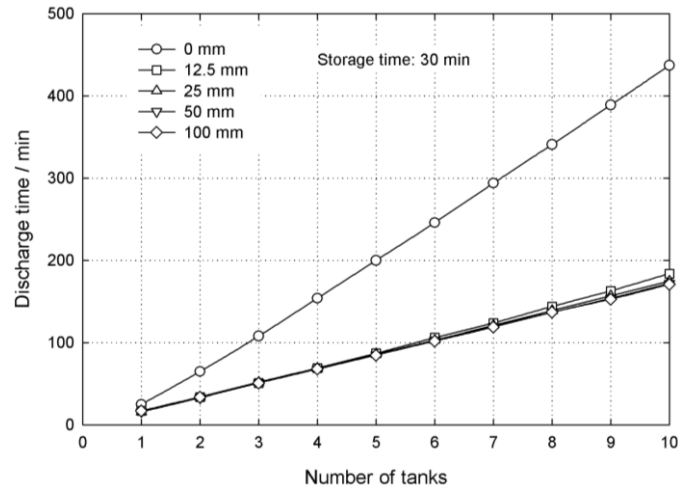
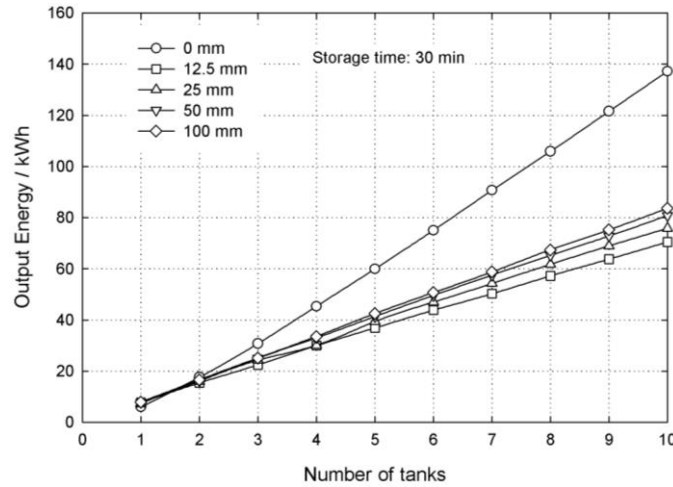


**Figure 4:** Discharge time vs number of tanks for a storage time of 30 min with different insulation thickness

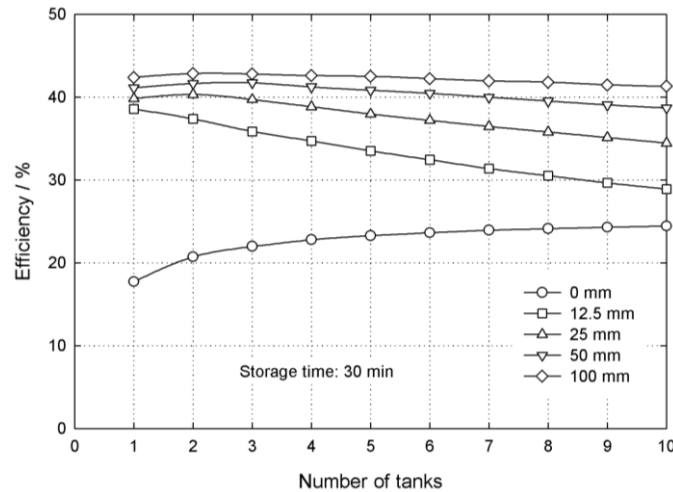
Figures 3 and 4 show the charge and discharge time performance, respectively, when the effect of the number of tanks and thickness insulation have been evaluated. It is possible to observe that when the tanks do not have insulation, their respective times are larger in both cases. The charge time without thermal insulation is increased because during the charge process the tank is cooled by heat transferred to the surroundings and it allows more mass to be stored until the maximum pressure is reached. So, the discharge time is increased proportionally because more mass was stored and it takes more time to empty the tank. Related to the charge and discharge time, the insulation thickness does not have a significant effect as is shown, nevertheless when the number of tanks is increased the charge and discharge time increases because more mass can be stored.

Figure 5 and Figure 6 show the output energy and efficiency, respectively, when the effect of the number of tanks and thickness insulation has been evaluated. According to the results previously shown, the output energy is increased as the number of tanks increases since more mass has been stored and it causes more energy to be in the tank. Contrary to what could have been expected, when the tanks are thermally insulated the output energy is decreased significantly, this is caused because less mass has been stored, also if the thickness of insulation is increased, less heat losses are present in the storage process and more energy is recovered, however, the increase in output energy when the insulation thickness is increased is very low. The efficiency of the system, defined as the ratio of the energy delivered by the generator to the energy consumed by the motor, is increased when the thickness insulation is bigger as shown in Figure 6. In this case the lower efficiency is presented when the system does not have insulation,

it is because more energy is dissipated to the environment and lower output energy is obtained, reducing thus the efficiency.

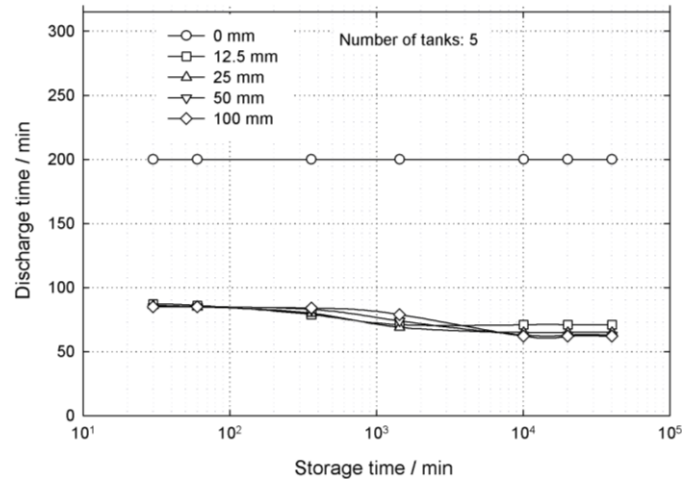


**Figure 5:** Output energy vs number of tanks for a storage time of 30 min with different insulation thickness



**Figure 6:** Efficiency vs number of tanks for a storage time of 30 min with different insulation thickness

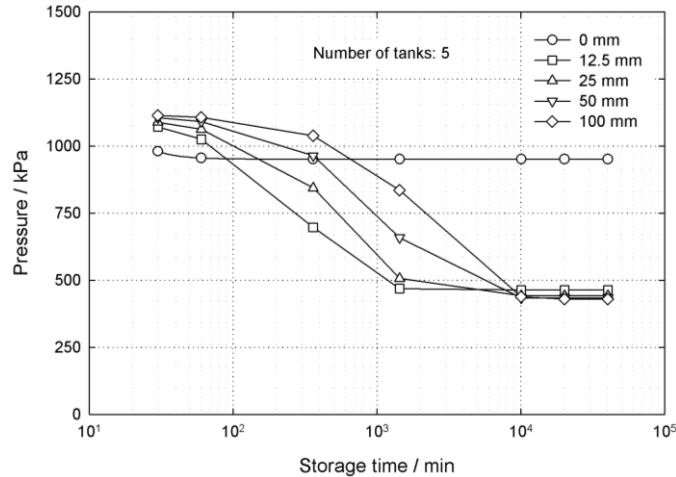
From Figure 7 to Figure 11 the effect of increasing the storage time in the operational parameters of the system is shown. The storage time was varied from zero minutes to one month by increments of one minute by maintaining the extraction mass flow rate constant and equal to the supply mass flow rate for a storage system consisting of five tanks. These numbers of tanks was chosen for this analysis because for this number of tanks without insulation the efficiency starts to be constant and shows the maximum value.



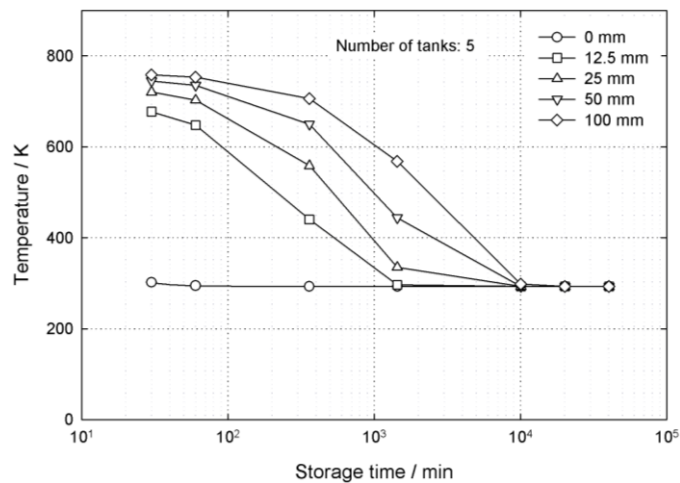
**Figure 7:** Discharge time vs storage time for a storage system consisting of five tanks with different insulation thickness

Figure 7 shows the discharge time versus the storage time and insulation thickness. It can be observed that the larger discharge time occurs when the tanks do not have insulation and it is basically constant. This behavior is due to the fact that without insulation, the air temperature at the end of the storage process is basically the same as the ambient temperature (a difference about 10 degrees) and the energy losses in the systems are almost zero. On the other hand, when the tanks are insulated, the discharge time decreases smoothly until reaching a constant discharge time which is independent of the storage time, it means that the tanks and the surroundings are in thermal equilibrium.

Figures 8 and 9 show the effect of increasing the storage time and insulation thickness on pressure and temperature of the stored air, respectively. Figure 8 shows that the air pressure decreases as the storage time increases until reaching a constant pressure which happens once the thermal equilibrium has been reached. This fact can also be noticed in Figure 9 where the evolution of air temperature respect to time confirms that the thermal equilibrium has been reached. Figures 8 and 9 also show that the higher air pressure and temperature are reached with the thicker insulation during the shorter times. Besides, the time needed to reach equilibrium changes from one day to one week with an insulation thickness of 12.5 mm and 100 mm, respectively.



**Figure 8:** Air pressure vs storage time for a storage system consisting of five tanks with different insulation thickness



**Figure 9:** Air temperature vs storage time for a storage system consisting of five tanks with different insulation thickness

Figure 10 and Figure 11 show the output energy and efficiency of the system, respectively, when the storage time is increased. The output energy is higher in the storage system without insulation, as shown in Figure 10. When the insulation effect is considered, the output energy is higher for a larger storage time (but less than around  $10^4$  min) as the insulation thickness increases. Once the storage system with insulated tanks reaches thermal equilibrium, the output energy is nearly independent of the insulation thickness and its magnitude is about one sixth of the output energy of a storage system without insulation.

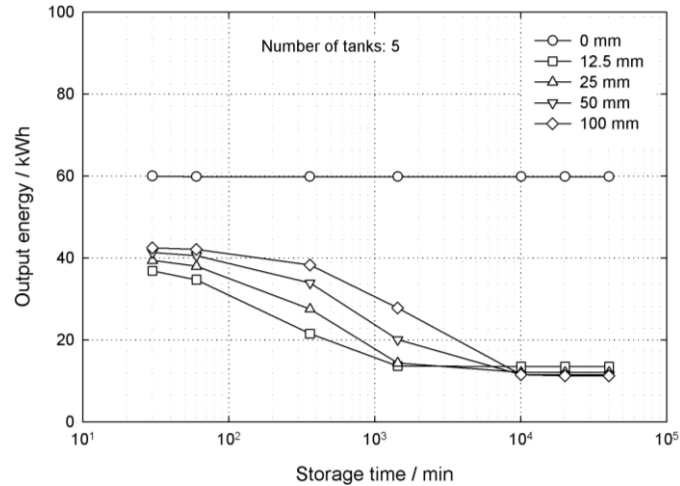


**Figure 10:** Output energy vs storage time for a storage system consisting of five tanks with different insulation thickness

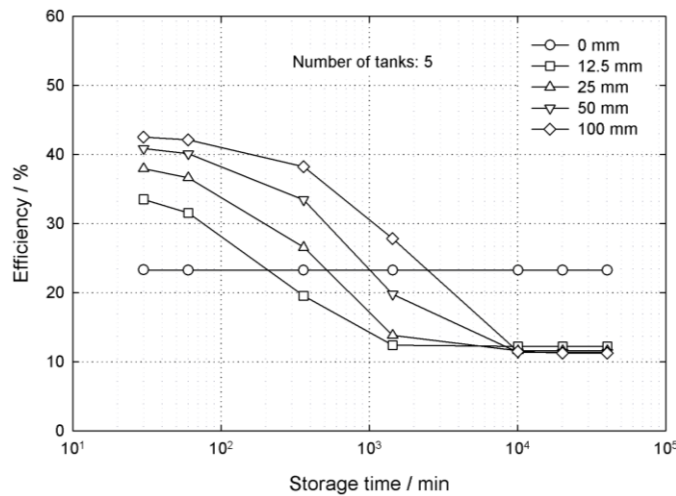


**Figure 11:** Efficiency vs storage time for a storage system consisting of five tanks with different insulation thickness

The efficiency of the system decreases as the storage time increases, as shown in Figure 11, but it increases by increasing the insulation thickness. The efficiency is kept almost constant at a high storage time being slightly higher for the smaller insulation thickness. It can be observed that the thicker the insulation, the longer the storage time at higher efficiency is maintained, facts that are quite expected. The efficiency of the tanks without insulation is almost constant and therefore basically independent of the storage time. When the equilibrium is reached by the storage system with insulation, the efficiency is almost half of the system efficiency without insulation. It means that it is more effective to use insulation when the storage time is short which is the opposite for a relatively long storage time.

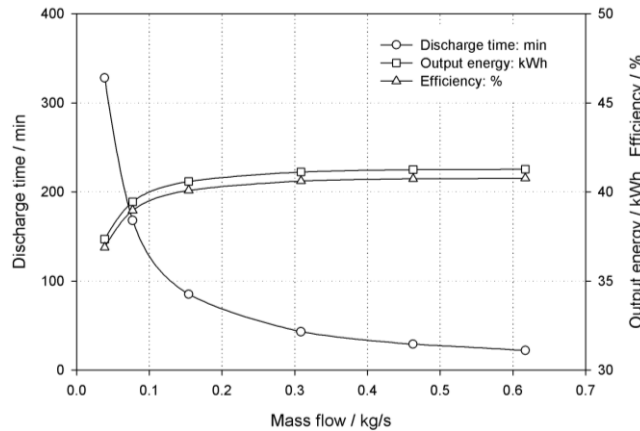


**Figure 12:** Variations in discharge time, energy output and efficiency respect mass flow

Finally, Figure 12 shows the effect of changing the outflow rate on the operational parameters. A storage system consisting of five tanks, with a storage time of one hour and an insulation thickness of 50 mm was selected. The results show that the discharge time is reduced significantly when the outflow rate is increased which causes an energy output increase since the turbine develops more power because it is proportional to the mass flow rate. As a consequence, the system efficiency increases.

Figure 1 showed that the mean consumption is 400 kWh, and for a period of 13 hrs corresponding from 6:00hrs to 19:00 hrs the demand is larger than the mean consumption for about 200 kWh. The previous analyses considered an array of 5 tanks connected in parallel which delivered a mean output energy of almost 40 kWh. A system capable of delivering 200 kWh needs to have 5 arrays connected in serial with each array consisting of 5 tanks connected in parallel. The operation of this system needs to consider the storage time by the array of tanks while the rest of the arrays are charged and discharged. For example, 5 tanks connected in parallel get fully charge in 81 minutes and they discharge in almost 84 minutes, it means that the first of the five arrays needs almost 6 hrs of storage time until the energy is used. The system described above is evaluated considering those factors and the total output energy is almost 191 kWh, with an efficiency of 38% and a discharge time of 7 hours. This system would provide the required energy for the hypothetical case during about half the time of the peak demand needed from 6:00 hrs to 19:00 hrs.

## 4. Conclusions

The transient analysis of the proposed CAES system shows that for short periods of storage time it is more convenient to use insulated tanks, whilst for long periods it is more convenient to use uninsulated tanks. The efficiency of the system is higher for short storage periods with insulated tanks, reaching efficiencies close to 42%, which are similar to the ones reported in literature (Luo, Wang, Dooner, & Clarke, 2015), (Budt, Wolf, Span, & Yan, 2016). Although the CAES system efficiency is lower than the efficiencies of other systems, e.g., battery storage systems whose efficiency is in the range of 75-90% (Luo, Wang, Dooner, & Clarke, 2015), (Budt, Wolf, Span, & Yan, 2016), most battery storage systems have small power capacities as compared to CAES systems. The CAES efficiency must be improved to use it in energy recovery systems as reported in the literature (Luo, et al., 2016), (Shakeri, Soltanzadeh, Berson, & Sharp, 2014), (Luo, Wang, Dooner, & Clarke, 2015), (Zhao, Wu, Hu, Xu, & Rasmussen, 2015), (Beaudin, Zareipour, Schellenberglabe, & Rosehart, 2010), (Budt, Wolf, Span, & Yan, 2016). The design of the system is enhanced when the irreversibilities and cost analysis are taken into account, hence, for future works exergy and thermoeconomic analysis will be considered. Also an auxiliary system can be considered to capture and re-use the heat during the compression and storage processes in order to increase the efficiency of the system.

## 5. Nomenclature

**Table 1: Symbols**

$\dot{m}$	Mass flow rate, kg/s
T	Temperature, K
P	Pressure, kPa
$\dot{W}$	Work rate, kW
$\dot{Q}$	Heat flow rate, kW
E	Energy, kWh
m	Mass, kg
t	Time, s
x	Mass fraction
k	Thermal conductivity, W/m-K



$l$	Thickness, m
A	Area, m <sup>2</sup>
C	Effective heat transfer coefficient, kW/m <sup>2</sup> -K
$h$	Specific enthalpy, kJ/kg /convective heat transfer coefficient, W/m <sup>2</sup> K
$s^o$	Specific entropy of ideal gas at standard pressure, kJ/kg-K
$y$	Independent variable
R	Universal gas constant.

**Table 2: Greek letters**

$\eta$	Efficiency, %
$\Delta$	Difference

**Table 3: Subscripts**

$\infty$	Environment conditions
1	Compressor inlet
2	Compressor exit
3	Turbine inlet
4	Turbine exit
C	Compressor
T	Turbine
max	Maximum
M	Motor
G	Generator
O <sub>2</sub>	Oxygen
N <sub>2</sub>	Nitrogen
i	Inlet
e	Exit
CV	Control volume
in	Motor inlet
out	Generator exit
dis	Dissipated

j	Time level
s	Isentropic

## References

- Akinyele, D. O., & Rayudu, R. K. (2014). Review of energy storage technologies for sustainable power networks. *Sustainable Energy Technologies and Assessments*, 8, 74-91.  
<https://doi.org/10.1016/j.seta.2014.07.004>
- Beaudin, M., Zareipour, H., Schellenberglabe, A., & Rosehart, W. (2010). Energy storage for mitigating the variability of renewable electricity sources: An updated review. *Energy for Sustainable Development*, 14, 302-314. <https://doi.org/10.1016/j.esd.2010.09.007>
- Budt, M., Wolf, D., Span, R., & Yan, J. (2016). A review on compressed air energy storage: Basic principles, past milestones and recent developments. *Applied Energy*, 170, 250-268. <https://doi.org/10.1016/j.apenergy.2016.02.108>
- Charan, C. R., Laxmi, A. J., & Sangeetha, P. (2017). Optimized Energy Efficient Solution With Stand Alone PV System. *MATTER: International Journal of Science and Technology*, 3. <https://dx.doi.org/10.20319/Mijst.2017.31.1627>
- de Boer, H. S., Grond, L., Moll, H., & Benders, R. (2014). The application of power-to-gas, pumped hydro storage and compressed air energy storage in an electricity system at different wind power penetration levels. *Energy*, 72, 360-370.  
<https://doi.org/10.1016/j.energy.2014.05.047>
- Guo, C., Xu, Y., Zhang, X., Guo, H., Zhou, X., Liu, C., . . . Chen, H. (2017). Performance Analysis of Compressed Air Energy Storage Systems Considering Dynamic Characteristics of Compressed Air Storage. *Energy*.  
<https://doi.org/10.1016/j.energy.2017.06.145>
- Hoffman, J. D., & Frankel, S. (2001). *Numerical methods for engineers and scientists*. CRC press.
- Huang, Y., Keatley, P., Chen, H. S., Zhang, X. J., Rolfe, A., & Hewitt, N. J. (2017). Techno-economic study of compressed air energy storage systems for the grid integration of wind power. *International Journal of Energy Research*. <https://doi.org/10.1002/er.3840>
- Jannelli, E., Minutillo, M., Lavadera, A. L., & Falcucci, G. (2014). A small-scale CAES (compressed air energy storage) system for stand-alone renewable energy power plant for

- a radio base station: A sizing-design methodology. *Energy*, 78, 313-322.  
<https://doi.org/10.1016/j.energy.2014.10.016>
- Kaya, M., Tari, I., & Baker, D. K. (2016). Numerical Comparison and Sizing of Sensible and Latent Thermal Energy Storage for Compressed Air Energy Storage Systems. ASME 2016 International Mechanical Engineering Congress and Exposition, (págs. V06BT08A048--V06BT08A048). <https://doi.org/10.1115/IMECE2016-66145>
- Klein, S. A., & Nellis, G. (2013). Mastering EES. F-Chart Software.
- Luo, X., Wang, J., Dooner, M., & Clarke, J. (2015). Overview of current development in electrical energy storage technologies and the application potential in power system operation. *Applied Energy*, 137, 511-536. <https://doi.org/10.1016/j.apenergy.2014.09.081>
- Luo, X., Wang, J., Krupke, C., Wang, Y., Sheng, Y., Li, J., . . . Chen, H. (2016). Modelling study, efficiency analysis and optimisation of large-scale Adiabatic Compressed Air Energy Storage systems with low-temperature thermal storage. *Applied energy*, 162, 589-600. <https://doi.org/10.1016/j.apenergy.2015.10.091>
- Mahlia, T. M., Saktisahdan, T. J., Jannifar, A., Hasan, M. H., & Matseelar, H. S. (2014). A review of available methods and development on energy storage; technology update. *Renewable and Sustainable Energy Reviews*, 33, 532-545. <https://doi.org/10.1016/j.rser.2014.01.068>
- Mancherter Tank Co. (2017). Obtenido de <http://www.mantank.com/>
- Moran, M. J., Shapiro, H. N., Boettner, D. D., & Bailey, M. B. (2010). *Fundamentals of engineering thermodynamics*. John Wiley & Sons.
- Nikolakakis, T., & Fthenakis, V. (2017). The Value of Compressed-Air Energy Storage for Enhancing Variable-Renewable-Energy Integration: The Case of Ireland. *Energy Technology*. <https://doi.org/10.1002/ente.201700151>
- Rogers, A., Henderson, A., Wang, X., & Negnevitsky, M. (2014). Compressed air energy storage: Thermodynamic and economic review. PES General Meeting| Conference \& Exposition, 2014 IEEE, (págs. 1-5). <https://doi.org/10.1109/PESGM.2014.6939098>
- Shakeri, M., Soltanzadeh, M., Berson, R. E., & Sharp, M. K. (2014). Comparison of Energy Storage Methods for Solar Electric Production. ASME 2014 8th International Conference on Energy Sustainability collocated with the ASME 2014 12th International Conference on Fuel Cell Science, Engineering and Technology, (págs. V001T02A008--V001T02A008). <https://doi.org/10.1115/ES2014-6347>

- Soltan, B. K., & Thorman, B. (2017). Building Energy Systems Operation Optimization with Ice Storage--A Real Time Approach. *MATTER: International Journal of Science and Technology*, 3.
- Szablowski, L., Krawczyk, P., Badyda, K., Karellas, S., Kakaras, E., & Bujalski, W. (2017). Energy and exergy analysis of adiabatic compressed air energy storage system. *Energy*. <https://doi.org/10.1016/j.energy.2017.07.055>
- Yang, Z., Wang, Z., Ran, P., Li, Z., & Ni, W. (2014). Thermodynamic analysis of a hybrid thermal-compressed air energy storage system for the integration of wind power. *Applied Thermal Engineering*, 66, 519-527. <https://doi.org/10.1016/j.applthermaleng.2014.02.043>
- Zhao, H., Wu, Q., Hu, S., Xu, H., & Rasmussen, C. N. (2015). Review of energy storage system for wind power integration support. *Applied Energy*, 137, 545-553. <https://doi.org/10.1016/j.apenergy.2014.04.103>
- Zhao, P., Gao, L., Wang, J., & Dai, Y. (2016). Energy efficiency analysis and off-design analysis of two different discharge modes for compressed air energy storage system using axial turbines. *Renewable Energy*, 85, 1164-1177. <https://doi.org/10.1016/j.renene.2015.07.095>